Low-Energy Hot Plasma and Particles in Saturn's Magnetosphere

Abstract. *The low-energy charged particle instrument on Voyager 2 measured low-energy electrons and ions (energies ⩾ 22 and ⩾ 28 kiloelectron volts, respectively) in Saturn's magnetosphere. The magnetosphere structure and particle population were modified from those observed during the Voyager 1 encounter in November 1980 but in a manner consistent with the same global morphology. Major results include the following. (i) A region containing an extremely hot (~ 30 to 50 kiloelectron volts) plasma was identified and extends from the orbit of Tethys outward past the orbit of Rhea. (ii) The low-energy ion mantle found by Voyager 1 to extend ~ 7 Saturn radii inside the dayside magnetosphere was again observed on Voyager 2, but it was considerably hotter (~ 30 kiloelectron volts), and there was an indication of a cooler (< 20 kiloelectron volts) ion mantle on the nightside. (iii) At energies ⩾ 200 kiloelectron volts per nucleon, H, H_2, and H_3 (molecular hydrogen), helium, carbon, and oxygen are important constituents in the Saturnian magnetosphere. The presence of both H_2 and H_3 suggests that the Saturnian ionosphere feeds plasma into the magnetosphere, but relative abundances of the energetic helium, carbon, and oxygen ions are consistent with a solar wind origin. (iv) Low-energy (~ 22 to ~ 60 kiloelectron volts) electron flux enhancements observed between the* L *shells of Rhea and Tethys by Voyager 2 on the dayside were absent during the Voyager 1 encounter. (v) Persistent asymmetric pitch-angle distributions of electrons of 60 to 200 kiloelectron volts occur in the outer magnetosphere in conjunction with the hot ion plasma torus. (vi) The spacecraft passed within ~ 1.1° in longitude of the Tethys flux tube outbound and observed it to be empty of energetic ions and electrons; the microsignature of Enceladus inbound was also observed. (vii) There are large fluxes of electrons of ~ 1.5 million electron volts and smaller fluxes of electrons of ~ 10 million electron volts and of protons ⩾ 54 million electron volts inside the orbits of Enceladus and Mimas; all were sharply peaked perpendicular to the local magnetic field. (viii) In general, observed satellite absorption signatures were not located at positions predicted on the basis of dipole magnetic field models.*

The primary scientific objectives of the low-energy charged particle (LECP) investigation in the magnetosphere of Saturn are to determine the intensity, energy spectra, composition, angular distributions, and spatial and temporal characteristics of ions ($E \geqslant 28$ keV) and electrons ($E \geqslant 22$ keV), with special attention to the interactions of these particle populations with the satellites (Titan, Rhea, Dione, Tethys, Enceladus, and Mimas) and rings (especially the E ring) in the magnetosphere. The trajectory for Voyager 2 enabled us to investigate the magnetosphere of Saturn at generally higher latitudes than was possible during the flyby of either Voyager 1 or Pioneer 11; in addition, Voyager 2 approached closer to the planet, ~ 2.67 Saturn radii (R_S), than did Voyager 1. The LECP instrument has two sensor systems: the low-energy particle telescope (LEPT) and the low-energy magnetospheric particle analyzer (LEMPA), both of which have a large number of solid-state detectors that can be used in various coincidence-anticoincidence configurations. A full description of the LECP has been given elsewhere (*1*, *2*).

Overview. Figure 1 provides a summary of particle intensities at several energies for the entire Voyager 2 encounter. The electron intensities (Fig. 1A) are dominated by the low energies (~ 22 keV) at the magnetopause, as was also noted by Voyager 1, when the magnetopause was beyond Titan's orbit (*3*). Inbound, the low-energy electrons begin decreasing in intensity outside Rhea's orbit, a decrease which continues up to the time of spacecraft closest approach, with the exception of an increase between the orbits of Rhea and Tethys. The electron intensity is greatly enhanced outbound and peaks in the region between Rhea and Dione; it then decreases by ~ 10^3 outside ~ 13 R_S. The intensity profile of intermediate (~ 250 keV) electrons (Fig. 1A) behaves differently; both inbound and outbound the maximum fluxes occur near the magnetic L shell of Dione. There is not yet clear evidence for a flux of such electrons inside the orbit of Mimas. Outbound, the higher energy electron intensity decreased to near background by ~ 13 R_S. The high-energy (~ 80 MeV) protons (Fig. 1A) are present only inside the orbits of Enceladus and Mimas, as also found by Pioneer 11 (*4–7*).

Even taking into account the fact that the outbound trajectory was on the predawn sector (see Fig. 5), Voyager 2 found the magnetosphere to be asymmetric beyond ~ 10 R_S in both high- and low-energy electron fluxes. Outbound, substantial activity in the low- and intermediate-energy electrons was observed all the way to the vicinity of the magnetopause crossings (~ 50 R_S) and throughout the magnetosheath.

Several ion channels, covering an energy range from ~ 30 keV to ~ 2 MeV, are shown in Fig. 1B. Increased fluxes of low-energy ions are present immediately preceding the first bow shock crossing and are modulated by the successive encounters of the spacecraft with the bow shock. The magnetopause crossing occurred inside the orbit of Titan; strong, energy-dependent signatures are apparent in the intensity of the ions throughout the encounter, with a clear change in the profiles at ~ 13 R_S, where the intensities at lower ion energies drop abruptly; then all channels begin a steady increase. Below we establish that this is the boundary between an outer mantle of low-energy ions, as seen by Voyager 1 (*3*), and another feature, an inner hot plasma torus. Satellite absorption effects are most evident at the higher energies, where the intensity of 1-MeV ions shows a gradual decrease across the orbit of Dione. Satellite effects for lower energy ions are clearly evident, but much less pronounced than at higher energies.

The ion intensity profiles between the inbound and outbound trajectories appear generally symmetric inside ~ 10 R_S but quite asymmetric outside ~ 13 R_S. A change in the slope of the intensity profiles is evident outbound at a distance of ~ 13 R_S, close to the L shell of the inbound boundary of the mantle region. No marked intensity signatures are evident outbound at the estimated crossing of the Titan L shell. The intensity profile beyond this distance is probably dominated by time variations, with large intensity fluctuations continuing past the magnetopause into the magnetosheath and beyond the bow shock encounters. Large ion increases (not shown) have been observed to distances of at least 250 R_S downstream from the planet.

Inner magnetosphere. Figure 2 shows data obtained from LEMPA while the instrument was in its near-encounter mode close to the planet (*1*). In this mode the instrument uses fast (20 to 50 nsec pulse widths) electronics, including fast coincidence techniques, to measure electrons in the range of ~ 1 to ~ 20 MeV and protons in the range of ~ 16 to ~ 150 MeV, as well as the normal complement of lower energy ions and electrons. The top curve in Fig. 2C shows 4-minute averages of the intensities of electrons ($E \geqslant 1.5$ MeV). Clear signatures of satellite L shell crossings are not

 0036-8075/82/0129-0571$01.00/0

evident on this time scale for such electrons. The intensities of electrons with energy ≥ 10 MeV (Fig. 2C, middle curve) exhibit clear discontinuities in the vicinities of the crossings of various satellite L shells; the location of the L shells are calculated on the basis of a centered, nontilted dipole. Intensity profiles of energetic protons (Fig. 2C, bottom curve) in the indicated energy interval show discontinuities at the satellite L shell crossings of Enceladus and Mimas, as was observed during the Pioneer experiments (*4–7*). Both the middle and bottom curves in Fig. 2C exhibit substantial variability, resulting from instrument scanning during the averaging interval (4.0 minutes) and relatively poor counting statistics.

The predicted L shell crossings (Fig. 2C) appear to be in general agreement with the observed signatures in the energetic proton intensities. There are, however, discrepancies that are illustrated in the high time resolution (400 msec per data point) intensity profiles of ~ 1.5-MeV electrons observed at the orbit of Enceladus (Fig. 2A) and Tethys (Fig. 2B). The Enceladus microsignature occurs later than expected, and the Tethys microsignature is observed some 4 minutes earlier than the predicted L shell crossing. The spacecraft passed extremely close (≤ 1.1° in longitude) to the Tethys flux tube; the observed microsignature is well defined. The width of the signature, taking into account the spacecraft velocity, results in a spatial dimension of ~ 10^3 km, which is comparable to the diameter of Tethys (~ 1050 km). The Enceladus and Tethys microsignatures were observed to extend in energy from a few tens of kiloelectron volts for electrons to ~ 2 MeV for protons. These observations indicate that the predictive capability of Saturnian magnetic field models may well depend on the instantaneous state of Saturn's magnetosphere.

Data on low-energy particles are not shown because of the need for detailed corrections due to penetrating background radiation. Preliminary analysis, however, suggests that energetic (≥ 200 keV) ions are not likely to be present in large numbers inside the orbit of Mimas (*5*).

Energy spectra. Figure 3 shows a summary of the spectral variations of both ions and electrons observed during the main part of the encounter. Ion energy spectra cover the range of ~ 28 keV to ~ 4 MeV (Fig. 3A). For the period shown, the spectra cannot be described by a power law in energy, since they bend toward lower energies, a characteristic of hot Maxwellian distributions (*8*). The similarity in spectral shapes at E ≤ 200 keV between the magnetosheath and outer magnetosphere suggests that the magnetosheath population may have been a part of the magnetosphere in the recent past, and is perhaps a remnant left by the inbound motion of the magnetopause just before spacecraft entry into the magnetosphere. Characteristic ion temperatures in the outer magnetosphere are in the range of ~ 20 to 30 keV.

As noted from the intensity profile in Fig. 1, the spectral shape changes substantially at ~ 1600 UT on day 237 at L ~ 13 R_S, with a depletion of fluxes below ~ 140 keV. At ~ 2300 UT, the spectrum becomes substantially softer and resembles a power law. Another notable feature is the depletion of higher (≥ 140 keV) energy fluxes inside the orbits of Dione and Tethys. Maxwellian fits (*9*) to the distribution functions result in characteristic ion temperatures in the range 40 to 55 keV, with the highest temperatures observed in the inbound L range of ~ 13 to ~ 7 R_S—that is, encompassing the Rhea L shell and extending to the L shell of Dione. Close inspection of Fig. 3B reveals a similar, but less extensive, high-temperature spectral feature during the outbound trajectory in the L range of ~ 6 to ~ 10 R_S. Detailed fits to the spectra show temperatures kT ~ 35 to 45 keV (where k is the Boltzmann constant and T is temperature), with the maximum value ~ 45 keV observed at L~ 7.7 R_S. Temperatures decrease at L ≥ 10 R_S and are ≤ 14 keV at L ≥ 12 R_S.

This region of high-temperature ions is similar in spatial extent to the plasma torus between the L shells of Rhea and Tethys discovered by Pioneer 11 (*10*), and is labeled provisionally the "hot plasma torus." It should be noted that similar spectral signatures were observed by the LECP instrument on Voyager 1, with the onset of high temperatures at L ~ 17 R_S marking the transition between the outer magnetosphere low-energy mantle and the region of stable trapping (*3*).

Energy spectra for electrons in the range ~ 22 to ~ 300 keV (Fig. 3B) are consistent with a power law in energy immediately after entry into the magnetosphere; the spectra gradually become harder as the spacecraft made its closest approach. Notable features of the spectra include the undulation in the intensity profile in the outer magnetosphere and, most important, the large enhancement in fluxes at low (≤ 60 keV) energies in the vicinity of the crossing of the L shells of Rhea through Dione. Such enhancement was not observed during the Voyager 1 encounter. Examination of data at higher (≥ 250 keV) energies (not shown) reveals a marked change in the electron

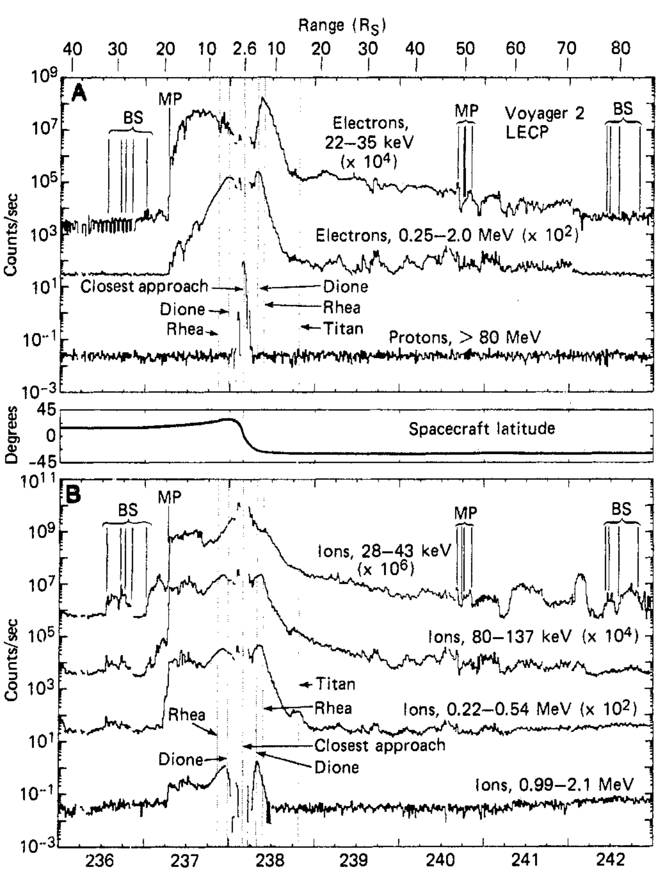

Fig. 1. Fifteen-minute averages of selected LECP channels. Bow shock (*BS*) and magnetosphere (*MP*) encounters are from Ness *et al.* (*22*). Dotted lines indicate crossings of outer satellite dipole L shells.

spectrum at ~ 350 keV, as the spacecraft approached the Rhea L shell; this change persisted through spacecraft closest approach but was not discernible after the outbound crossing of Rhea's L shell.

Composition of energetic particles. The composition measurements made with the LEPT sensor of the LECP experiment on Voyager 2 revealed considerably more information than similar measurements made from Voyager 1. The most abundant low-mass species in the energy range near 1 MeV per nucleon in the outer magnetosphere (Fig. 4A) are H, H_2, and He, as was also observed by Voyager 1 (*3*). There is, however, also an indication of the presence of H_3 molecules, although the statistics are limited (nine H_3 counts). Energetic H_3^+ molecular ions, which were abundant in Jupiter's magnetosphere (*11*), were absent from the Voyager 1 Saturn data.

Another difference during the Voyager 2 flyby was the presence of enhanced fluxes of heavier ions ≳ 0.2 MeV per nucleon. Heavy ions above this energy threshold were not present at the time of the Voyager 1 flyby. The presence of these heavy ions, as well as the H_3^+ ions, is consistent with the fact that the maximum ion energy in the outer magnetosphere was somewhat higher during the Voyager 2 encounter (~ 4 MeV total kinetic energy) than during the Voyager 1 encounter (~ 2 MeV).

At these low energies, the individual heavy elements are not well resolved, but the most abundant species may be identified. In Fig. 4B, the solid line shows the heavy ions detected in Saturn's magnetosphere over a 10-hour period during the inbound pass. The most abundant species are carbon and oxygen. For comparison, a similar histogram of data collected during a solar particle event several days before the encounter is shown as a dashed line. The overall distributions are similar, indicating similar heavy ion composition, except for the relatively higher carbon abundance in the magnetosphere. Also of interest is the nitrogen abundance, because of the possibility that Titan's atmosphere is a contributor of plasma to the magnetosphere. We conclude from Fig. 4B that nitrogen is no more abundant in the energetic magnetospheric particles than in the solar particles; this limits its abundance to ~ 20 percent that of oxygen.

The energy spectra of the low-mass species near 1 MeV per nucleon were similar to those from Voyager 1 (*3*) and may be characterized as steep power laws with spectral indices of ~ 6 for H and He and ~ 16 for H_2, with H_2 becoming more abundant than He below ~ 0.7

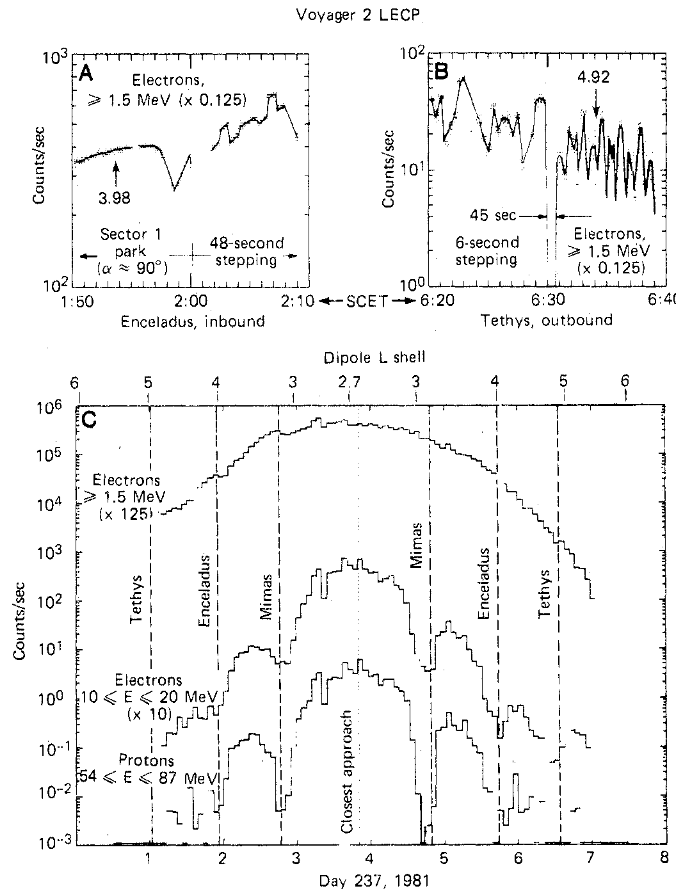

Fig. 2. (A and B) High-time resolution (400 msec) electron rates near two satellites, and (C) 4-minute averages of selected near-encounter LEMPA channels. Satellite dipole L shells are indicated by dotted lines in (C). Each dot in (A and B) represents data accumulated in 400-msec samples; solid lines have been drawn to show the overall trend in the data. Arrows indicate expected satellite dipole L shell crossings.

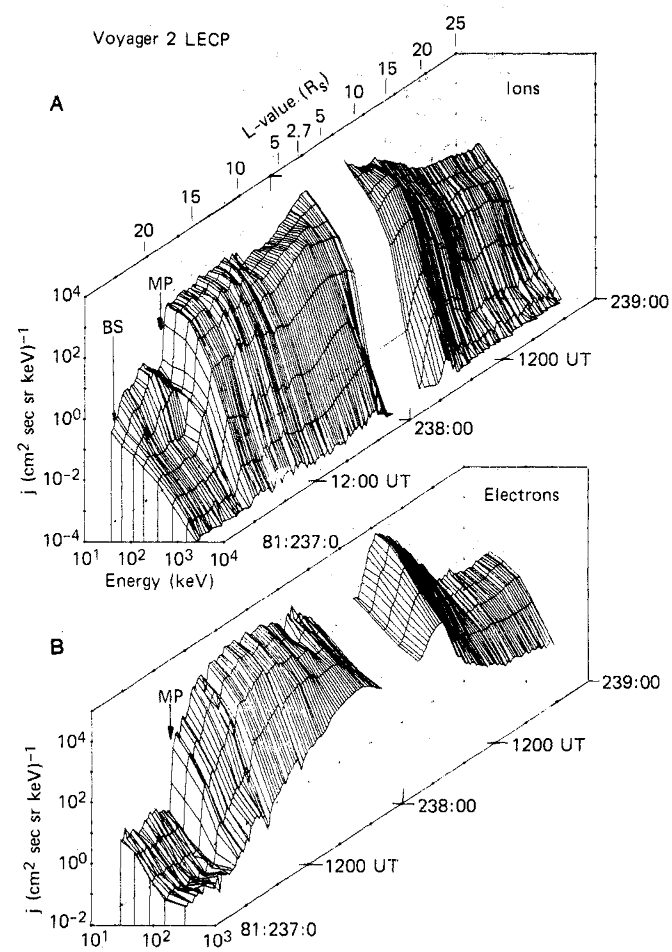

Fig. 3. Fifteen-minute averaged, three-dimensional differential flux (j) spectra of (A) ions and (B) electrons. Spectra near closest approach are not shown due to high background radiation in some channels. The last bow shock (*BS*) and the inbound magnetopause (*MP*) crossings are shown.

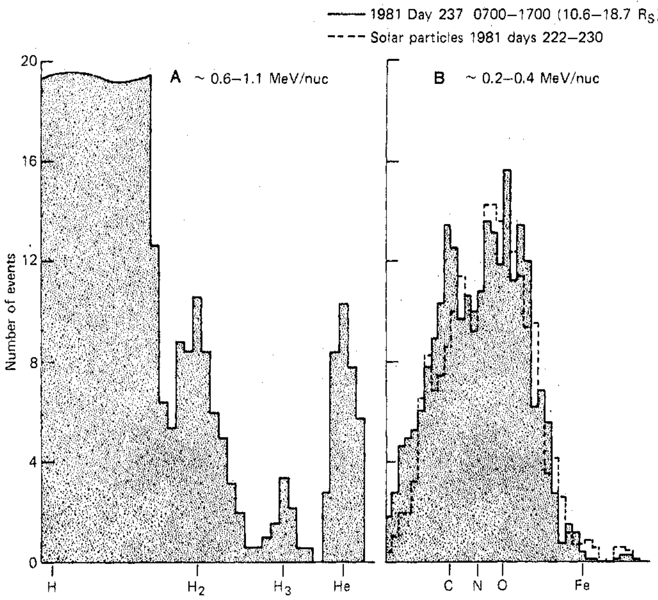

Fig. 4. (A) Mass histogram of light ions in Saturn's magnetosphere showing peaks at H, H_2, H_3, and He. (B) Mass histogram of heavier ions over the same time interval at somewhat lower energy per nucleon. Peaks are seen at carbon and oxygen. A similar histogram of solar particles is shown as a dashed line. The flux of heavy ions increased by more than a factor of 10 when Voyager 2 entered Saturn's magnetosphere.

MeV per nucleon. At equal energy per nucleon, the relative abundances of H, He, C, and O are roughly 54000:90:1:1. The relative He, C, and O abundances are typical of solar material. The H/He ratio (~ 600), however, is some 25 times higher than is typical for the solar wind. The extremely soft energy spectra, and the large ion fluxes inside the magnetosphere when compared to the nearby interplanetary medium, make it very unlikely that the observed He, C, and O fluxes were remnants of a solar flare particle event.

Anisotropies. Figure 5 presents the amplitudes and directions of the first order harmonic vectors derived from a Fourier representation of hourly average data plotted on the spacecraft trajectory. This representation uses data in the instrument scan plane, which is approximately parallel to the Saturnian equatorial plane on the inbound trajectory (Fig. 5, right upper inset). The instrument scan plane was inclined at a large (~ 60°) angle to the Saturnian equatorial plane on the outbound trajectory, as indicated by the projected sector center lines. The abrupt change in the direction and amplitude of the anisotropy as the spacecraft enters and leaves the magnetosphere suggests that the anisotropies are good indicators of boundary crossings.

Because of the scan plane orientation, the range of pitch-angle samples is usually ~ 45° to 135° or less; nonetheless, Voyager 2 measures a remarkable new type of electron anisotropy that was not seen on Voyager 1. A persistent asymmetric pitch-angle distribution characterizes the ~ 60- to 200-keV electrons. These are depicted in Fig. 5 at the locations along the Voyager 2 orbit where they occurred. They represent an isotropic forward hemisphere with fluxes monotonically decreasing for pitch angles $\alpha > 90°$ (where $\alpha = 0°$ is along the B vector). The directions both inbound and outbound are consistent with a deficiency of electrons returning from the southern polar region, and hence a net streaming down the field lines into this region. Clearly some degree of weak scattering is required to destroy the conservation of the magnetic moment of these electrons. The asymmetric electron distributions occur in the regions we identified (from Fig. 3) as the hot (kT ~ 50 keV) plasma torus (inbound and outbound) and the soft (< 20 keV) ion component (outbound), both within the temporal electron events (day 237, 2100 UT to day 238, 0000 UT) and the large low-energy electron intensity peak (day 238, 0600 to 1500 UT). The ions of about the same energies (137 to 215 keV) show no significant streaming inbound; their pitch-angle distributions are a complex combination of a second-harmonic pancake dis-

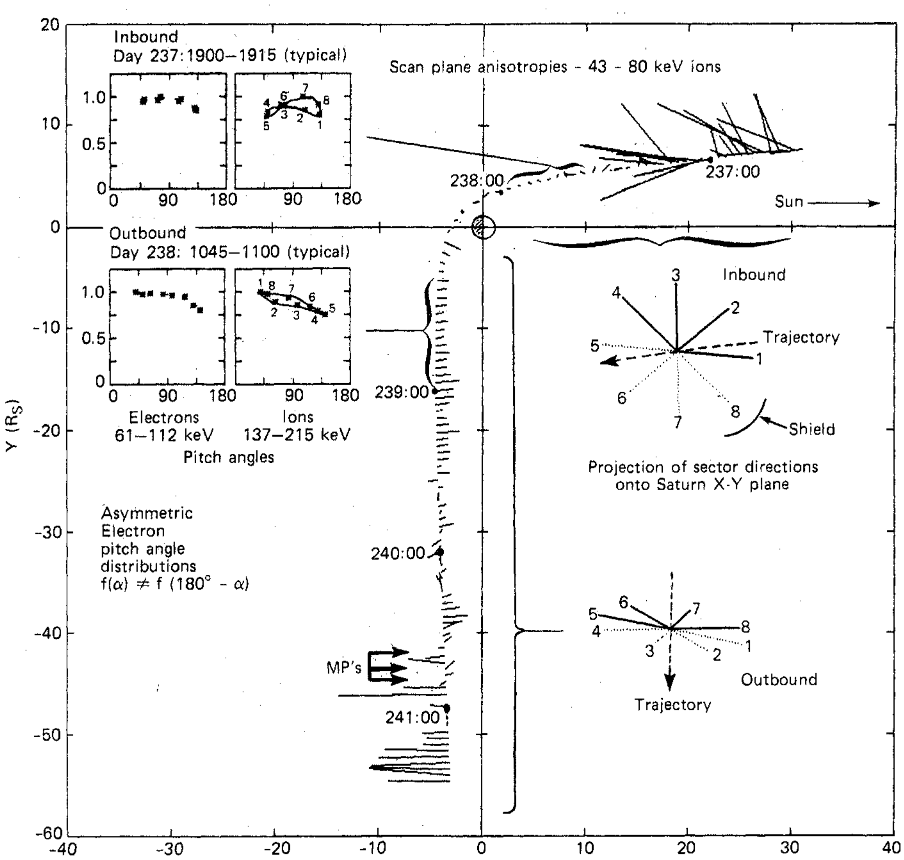

Fig. 5. First-order anisotropies along Voyager's trajectory. Each vector represents a 1-hour average of the anisotropy as measured in the LECP scan plane. The two insets on the right show the look directions of the instrument sectors projected onto the spin (xy) plane of Saturn. Solid sector lines indicate the sectors viewed above the plane; dotted lines indicate the sectors viewed below the plane; and dashed lines indicate relative spacecraft motion. The sudden increase in anisotropy amplitude after local midnight is an artifact of the reorientation of the spacecraft. Insets on the left show pitch-angle distributions (15-minute averages normalized to the sector of highest intensity) of 61- to 112-keV electrons and 137- to 215-keV ions. Although distributions are variable, those shown are representative of the forms most often observed on the portions of the orbit indicated by brackets.

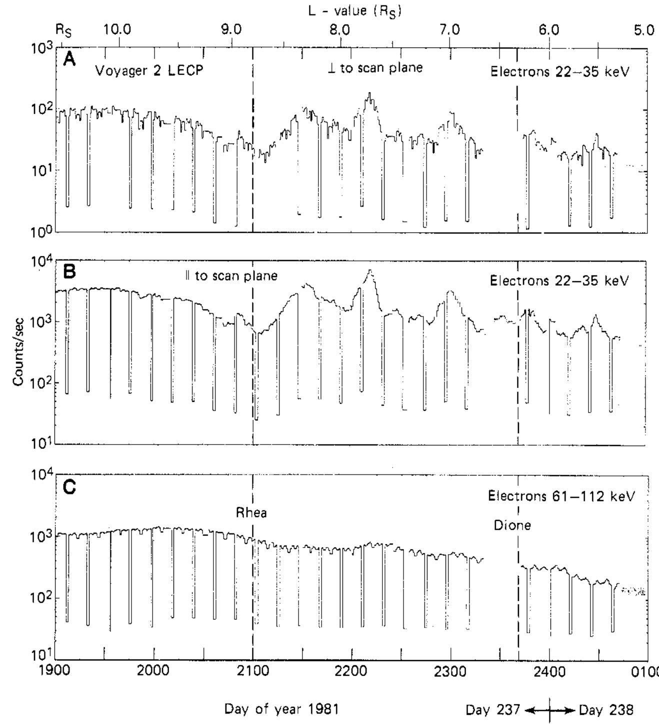

Fig. 6. Sector average rates for the "acceleration event." Each datum represents a 48-second average corresponding to a different sector look direction, or pitch angle (see inset in Fig. 5). The severe dropouts occurring every 16 sectors are due to the detectors' rotating behind the shield in sector 8. Near $L \sim 6.5$ R_S and ~ 5 R_S, the instrument operated in a nonstepping "park" mode. (A) Sector-averaged data from an electron detector which scans a pitch-angle range $\sim 11°$ to $122°$, that is, in a plane perpendicular to that of the normal instrument scan plane. (B) Sector-averaged intensities in the same energy range but from a detector which is generally viewing pitch angles close to $\sim 90° \pm 45°$, as deduced from the orientation of the instrument with respect to local magnetic field (*22*) during this time interval. (C) Higher energy electrons (60 to 112 keV) which display typical, trapped angular distributions.

tribution, some corotation convection, and possibly some field-aligned flow. The sampling sequence of sector positions (Fig. 5) is indicated in the ion pitch-angle representations. Both electron and ion anisotropies are highly variable inbound from the magnetopause to $L \sim 13$ R_S, from which we infer a somewhat disturbed magnetic field regime. Further analysis is required before we can describe the ion anisotropies definitively.

Evidence for electron acceleration. As noted, an unusual increase in the low-energy electron intensities occurred between the Rhea L shell and the Dione L shell on the inbound trajectory. This increase was limited in energy ($\lesssim 60$ keV) and displayed substantial fluctuations (apparently temporal) with order-of-magnitude changes in a few minutes. During the Voyager 1 encounter, the low-energy electron intensities were generally depressed in this region of space, even though the Voyager 1 trajectory was closer to the equatorial plane during the Rhea L shell crossing.

Figure 6 shows detailed electron intensity profiles for a 5-hour interval during which intensity fluctuations were observed. The electron intensity fluctuations are present in both low-energy detectors scanning in two mutually perpendicular directions (Fig. 6, A and B); similar intensities in both scan planes suggest a near isotropic pitch-angle distribution. The intensity fluctuations are interpreted as temporal, rather than spatial, since the low-energy angular distributions are not repetitive (such as those in Fig. 6C) and thus not characteristic of a steady-state distribution. The fluctuations begin close to the Rhea L shell, continue throughout this region past the Dione L shell, and appear to cease just before Tethys' L shell. No enhancements of low-energy electrons specifically associated with the Rhea and Dione L shells were observed during the outbound part of the trajectory (Fig. 1). However, significantly larger fluxes of energetic electrons were measured outbound (compared to inbound) between the Rhea and Dione L shells, even though the spacecraft trajectory at the orbit of Rhea is symmetric in B-L space inbound and outbound.

Discussion. The overall structure of the inner magnetosphere of Saturn seems to be dominated by the influence of Rhea and Mimas and, to a lesser extent, of Dione, Tethys, and Enceladus. The decrease in intensity of electrons inside the orbit of Rhea and the definite decrease in phase space density of energetic ions observed during the Voyager 1 encounter (*3*) has been related to the presence of a tenuous E ring in the equatorial plane of Saturn (*5, 12, 13*). However, these changes in phase space density of energetic ions and electrons also appear to occur in association with the presence of a torus-like region of plasma which extends from the orbit of Rhea to the orbit of Tethys (*10, 14*). In addition, this region of space is accompanied by intense, plasma wave emissions in the range of 1 to 5 kHz (*15*), which are reminiscent of the physical phenomena present in association with the Io plasma torus of Jupiter. Therefore, it may be possible that the decrease in the ion phase space densities which we observed with Voyager 1 is also associated with wave-particle interactions of an unspecified nature, in a manner analogous to that occurring in the vicinity of Io's torus (*16*). Additional support for this interpretation may be found in the Voyager 2 observation of what is, apparently, an electron acceleration event in association with the orbits of Rhea and Dione; this event is somewhat reminiscent of the electron acceleration observed in association with the traversal of the Io plasma torus by Pioneer 10 (*17*) and subsequently by Voyager 1 (*18*).

Concerning the magnetosphere inside the orbit of Mimas, we note that LECP data do not provide support for the presence of energetic ($\lesssim 4$ MeV) ions (< 30 cm^{-2} sec^{-1} sr^{-1}; $0.54 \leq E \leq 0.99$ MeV), as originally suggested by the results of Pioneer 11 (*4, 6*), although the presence of very low-energy ($\lesssim 200$ keV) ions and electrons has not been excluded. Substantial fluxes of high-energy protons (> 54 MeV) and electrons (1 to 20 MeV) are present inside the orbit of Mimas. Fillius and McIlwain (*7*) suggested that the origin of these high-energy protons is consistent with cosmic-ray interactions with the rings and the planetary atmosphere.

Of the six observed species of energetic ions (H, H_2, H_3, He, C, and O), only H_2, H_3, and He can be used as unambiguous tracers of their source. The hydrogen molecules H_2 and H_3 are presumably produced in the upper ionosphere of Saturn by nonequilibrium processes, such as energetic particle bombardment, and then are accelerated out of the auroral regions by, for example, parallel electric fields, as was also suggested to occur at Jupiter (*11*). In the case of Saturn, the atmosphere of Titan and the icy surfaces of several of the satellites could be additional sources of these molecules, although the absence of N and the presence of H_3 would argue against such a possibility. On the other hand, the solar wind is the likely source of the He ions since, under equilibrium conditions, ionospheric He is at too low an altitude to be readily accessible.

If the source of the He is solar, abundance ratios of C and O relative to He and to each other suggest that the energetic C and O ions might also be of solar wind origin, and hence highly ionized. On the other hand, direct measurements of the magnetospheric plasma have not indicated the presence of a large component with mass-to-charge ratio (A/Q) ~ 2. Frank *et al.* (*10*) deduced A/Q ~ 1, 5, and 8 for ions in various parts of the magnetosphere; they identified the ions as probably H^+, O^{3+}, and O^{2+}, respectively. Bridge *et al.* (*14*) identified a heavy ion component as either O^+ or N^+. Since there was no strong N component, Titan's atmosphere is an unlikely source of C and O. However, we cannot rule out a local origin, since it may be possible for C and O to be sputtered from the surfaces of the icy satellites (*19*) in roughly equal amounts and thus be present in the low-energy plasma. In this case, the solar-type abundance ratio of He (from the solar wind) to C and O (local) would be fortuitous.

When we summarize the Voyager 2 LECP observations of energy spectra, anisotropies, and composition (Fig. 7B) in the same manner as we did for Voyager 1 (Fig. 7A), we find a rather consistent and a somewhat clarified picture of the global characteristics of Saturn's outer magnetosphere. Comparing Fig. 7, A and B, we see several suggestions that the energetic particle population was in a more active state during the Voyager 2 encounter. The Voyager 2 dayside magnetopause was ~ 5 R_S closer to the planet than that observed by Voyager 1, and the ion mantle population, although having about the same equatorial thickness (~ 7 R_S) as found by Voyager 1, exhibited consistently higher intensities and a more rounded spectrum, characteristic of a hotter (kT ~ 25 keV) component (Fig. 3A), as opposed to the softer, power-law spectrum of Voyager 1. The disturbed magnetic field, which we infer from our anisotropy measurements, and the CNO/He abundance ratios typical of the solar wind add weight to our association of the ion mantle with a pseudotrapping region, probably of solar wind origin. Also, Voyager 2 observed a new, hot ion plasma torus (kT ~ 50 keV) in the region $7 \lesssim L \lesssim 13$ R_S inbound, and somewhat more limited in L outbound. Temporal electron events (inbound) and an anomalously high peak in the electron intensities outbound (inconsistent with inbound intensities in terms of B-L invariance) were also observed in this region. We find these signatures of hot ions and intense, time-varying fluxes of electrons to be highly reminiscent of the plasma sheet populations at Earth and Jupiter.

As Voyager 2 moved farther out on the nightside—it was still 58° tailward of the dawn terminator at 1200 UT on day 238—it encountered an ion population at southern latitudes whose spectrum above ~ 100 keV was similar to that seen by Voyager 1 at northern latitudes. However, Voyager 2 found a persistent enhancement in low-energy ions (kT < 15 keV) beginning at L ~ 12 R_S and continually observed throughout the next 36 hours (Fig. 3A). We speculate that this soft ion component may be the nightside manifestation of the dayside ion mantle, also occupying L shells above ~ 12 R_S. The reason why it may not have been observed by Voyager 1 outbound is that the dayside ion mantle was not as prominent at that time as it was for Voyager 2. Another significant difference between the two sets of observations is the low-energy electron and ion intensity dropouts observed by Voyager 1 in the post-midnight northern magnetotail but not observed by Voyager 2 in the predawn southern flank. In our Voyager 1 analysis (*3*), we noted that the dropouts coincided in subsolar longitude with the probable location of Saturn's auroral kilometric radiation. On

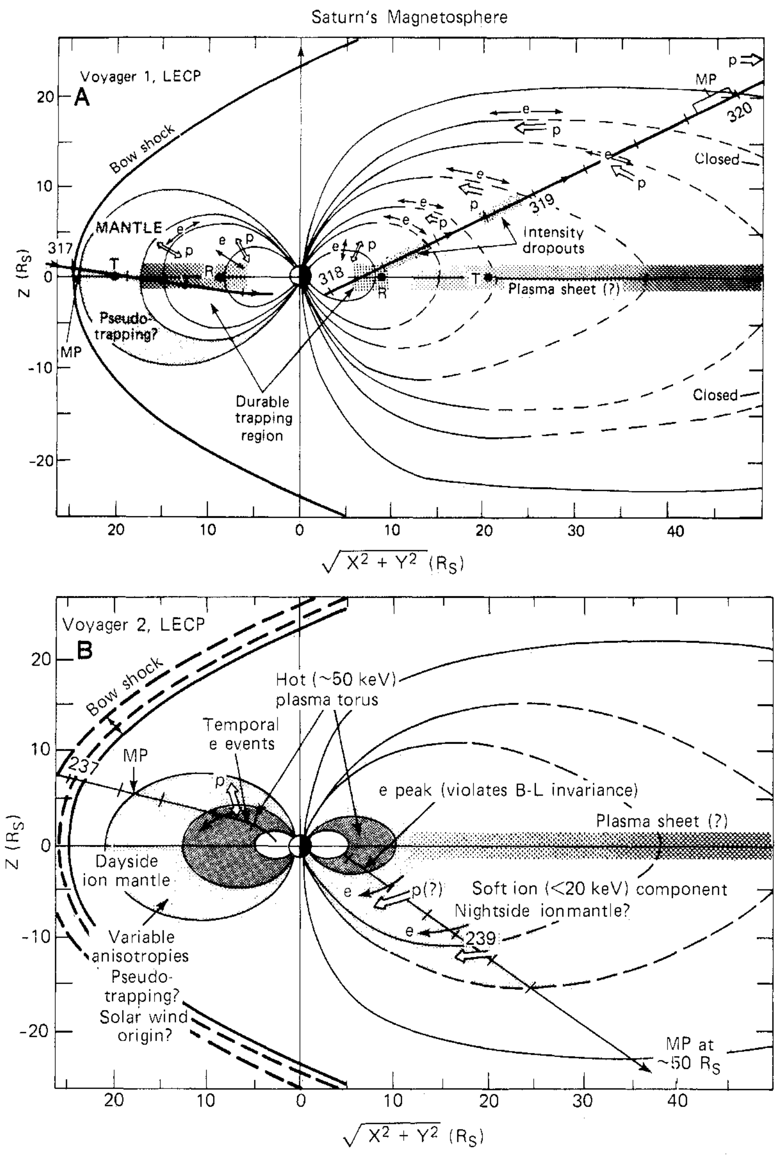

Fig. 7. (A) Sketch deduced from Voyager 1 LECP observations of global structure of energetic particle populations and circulation patterns in the outer magnetosphere [from (*3*)]. (B) Similar sketch deduced for Voyager 2. Note the following correspondences of Voyager 2 with Voyager 1: (i) dayside ion mantle pseudotrapping region has same thickness (~ 7 R_S) but is located ~ 4 R_S closer to planet; and (ii) electron streaming occurs in the same region as bidirectional cigar distributions for Voyager 1 on both day- and nightsides. New features seen by Voyager 2 include: (i) hot (kT ~ 30 to ~ 50 keV) ion population $6 < L < 13$ on both day- and nightsides; (ii) electron acceleration events (inbound) and intensity enhancement (outbound); (iii) possible nightside ion mantle identified by soft (≲ 30 keV) ion component; and (iv) magnetopause crossing farther out but no intensity dropouts en route to dawn flank. The general impression is of a higher energy particle population for Voyager 2.

the basis of their Voyager 1 measurements, Warwick *et al.* (*20*) and Kaiser *et al.* (*21*) conclude that the source of the strongest Saturnian kilometric radiation is located in the northern hemisphere. If there is a connection between such radiation and the particle dropouts, it may not be surprising that the dropouts were not observed by Voyager 2 since the outbound trajectory was in the southern hemisphere.

The north-south asymmetry in Saturnian kilometric radiation calls to mind the asymmetric electron pitch-angle distributions (Fig. 5), which represented a deficiency of ~ 60- to 200-keV electrons returning from the southern high latitude regions. Why were they not measured by Voyager 1? Comparing Fig. 7, A and B, we see that wherever Voyager 2 saw asymmetric pitch-angle distributions, inbound or outbound, Voyager 1 saw bidirectional cigar-shaped distributions. Thus the Voyager 1 cigar distributions may be manifestations of the same source, but with different boundary conditions near the polar regions.

In summary, if we allow for plausible differences in the dynamic state of Saturn's magnetosphere, the Voyager 1 and Voyager 2 energetic particle measurements complement each other and lead to a reasonably consistent global picture of a novel magnetosphere.

S. M. KRIMIGIS
Applied Physics Laboratory, Johns Hopkins University, Laurel, Maryland 20707
T. P. ARMSTRONG
Department of Physics, University of Kansas, Lawrence 66044
W. I. AXFORD
Max-Planck Institute for Aeronomy, D-3411 Katlenburg-Lindau 3, West Germany
C. O. BOSTROM
Applied Physics Laboratory, John Hopkins University
G. GLOECKLER
Department of Physics and Astronomy, University of Maryland, College Park
E. P. KEATH
Applied Physics Laboratory, Johns Hopkins University
L. J. LANZEROTTI
Bell Laboratories, Murray Hill, New Jersey 07974
J. F. CARBARY
Applied Physics Laboratory, Johns Hopkins University
D. C. HAMILTON
Department of Physics and Astronomy, University of Maryland
E. C. ROELOF
Applied Physics Laboratory, Johns Hopkins University

References and Notes

1. S. M. Krimigis, T. P. Armstrong, W. I. Axford, C. O. Bostrom, C. Y. Fan, G. Gloeckler, L. J. Lanzerotti, *Space Sci. Rev.* **21**, 329 (1977).
2. S. M. Krimigis, J. F. Carbary, E. P. Keath, C. O. Bostrom, W. I. Axford, G. Gloeckler, L. J. Lanzerotti, T. P. Armstrong, *J. Geophys. Res.* **86**, 8227 (1981).
3. S. M. Krimigis *et al.*, *Science* **212**, 225 (1981).
4. J. A. Simpson, T. S. Bastian, D. L. Chenette, R. B. McKibben, K. R. Pyle, *J. Geophys. Res.* **85**, 5731 (1980).
5. J. A. Van Allen, B. A. Randall, M. F. Thomsen, *ibid.*, p. 5679.
6. F. B. McDonald, A. W. Schardt, J. H. Trainor, *ibid.*, p. 5813.
7. W. Fillius and C. E. McIlwain, *ibid.*, p. 5803.
8. S. M. Krimigis *et al.*, *Science* **206**, 977 (1979).
9. S. M. Krimigis *et al.*, conference on "Physics of the Jovian and Saturnian Magnetospheres," Applied Physics Laboratory, Johns Hopkins University, Laurel, Md., 22 to 24 October 1981.
10. L. A. Frank, B. G. Burek, K. L. Ackerson, J. H. Wolfe, J. D. Mihalov, *J. Geophys. Res.* **85**, 5695 (1980).
11. D. C. Hamilton *et al.*, *Geophys. Res. Lett.* **7**, 813 (1980).
12. E. C. Sittler, Jr., J. D. Scudder, H. S. Bridge, *Nature (London)* **292**, 711 (1981).
13. A. Cheng, L. J. Lanzerotti, V. Pirronello, in preparation.
14. H. S. Bridge *et al.*, *Science* **212**, 217 (1981).
15. D. A. Gurnett, W. S. Kurth, F. L. Scarf, *ibid.*, p. 235.
16. D. A. Gurnett and F. L. Scarf, in *Physics of the Jovian Magnetosphere*, A. Dessler, Ed. (Cambridge Univ. Press, Cambridge, in press).
17. W. Fillius, in *Jupiter*, T. Gehrels, Ed. (Univ. of Arizona Press, Tucson, 1976), pp. 896–927.
18. S. M. Krimigis and E. C. Roelof, in *Physics of the Jovian Magnetosphere*, A. Dessler, Ed. (Cambridge Univ. Press, Cambridge, in press).
19. R. E. Johnson, L. J. Lanzerotti, W. L. Brown, T. P. Armstrong, *Science* **212**, 1027 (1981).
20. J. W. Warwick *et al.*, *ibid.*, p. 239.
21. M. L. Kaiser, M. D. Desch, A. Lacacheux, *Nature (London)* **292**, 731 (1981).
22. N. F. Ness, M. H. Acuña, R. P. Lepping, J. E. P. Connerney, K. W. Behannon, L. F. Burlaga, F. M. Neubauer, *Science* **215**, 558 (1982).
23. We thank the Voyager Project Office, JPL, and the Planetary Programs Office, NASA Headquarters, for help and cooperating in carrying out this experiment. We thank D. P. Peletier, S. A. Gary, R. G. King, J. W. Kohl, D. E. Fort, J. T. Mueller, J. H. Crawford, R. E. Thompson, B. A. Northrop, and J. Hook at APL/JHU; E. O. Tums, J. C. Cain, R. T. Cates, R. A. Lundgren, and D. C. Brown of the University of Maryland; C. G. Maclennan of Bell Laboratories; and J. O'Donnell, S. T. Brandon, and M. Paonessa of the University of Kansas for their enthusiasm and long hours that made the LECP experiment a success. The work of E. Franzgrote, O. Divers, and D. Griffith of JPL (among many others) was essential to the success of our investigation. We thank N. F. Ness and the MAG team for making their data available before publication. The LECP program was supported at APL/JHU by NASA under task I of contract N00024-78-C-5384 between Johns Hopkins University and the Department of the Navy and by subcontract at the universities of Kansas and Maryland.

10 November 1981

Energetic Charged Particles in Saturn's Magnetosphere: Voyager 2 Results

Abstract. *Results from the cosmic-ray system on Voyager 2 in Saturn's magnetosphere are presented. During the inbound pass through the outer magnetosphere, the ≥ 0.43-million-electron-volt proton flux was more intense, and both the proton and electron fluxes were more variable, than previously observed. These changes are attributed to the influence on the magnetosphere of variations in the solar wind conditions. Outbound, beyond 18 Saturn radii, impulsive bursts of 0.14- to > 1.0-million-electron-volt electrons were observed. In the inner magnetosphere, the charged particle absorption signatures of Mimas, Enceladus, and Tethys are used to constrain the possible tilt and offset of Saturn's internal magnetic dipole. At ~ 3 Saturn radii, a transient decrease was observed in the electron flux which was not due to Mimas. Characteristics of this decrease suggest the existence of additional material, perhaps another satellite, in the orbit of Mimas.*

The Saturn encounter trajectory of Voyager 2 provided a novel perspective from which to study the structure and dynamics of the Saturnian magnetosphere. Although Voyager 2, Voyager 1, and Pioneer 11 all entered the magnetosphere near the noon meridian, the Voyager 2 entry was at a latitude of 17°, significantly higher than either of the other spacecraft. As it approached Saturn, Voyager 2 traveled to ~ 30° latitude at 4 Saturn radii (R_S, 1 R_S = 60,330 km) before descending through the ring plane within the orbit of Mimas at 2.77 R_S. Outbound, the spacecraft left Saturn near the dawn meridian at a local time similar to that traversed by Pioneer 11 but at −30° latitude. The large latitude range and the close approach to Saturn are among the unique features of this trajectory which were exploited in this study of data obtained by the cosmic-ray system (*1*).

The outer magnetosphere. Voyager 2 entered Saturn's magnetosphere during a disturbed period when the solar wind pressure was highly variable (*2*). The fluxes of both energetic protons and electrons (Fig. 1) rose sharply ~ 15 minutes before the magnetopause crossing at 18.5 R_S (*2, 3*). Perhaps this precursor in the particle flux was related to the high latitude of the crossing or to magnetopause motion which may have kept Voyager 2 in the vicinity of the magnetopause for 15 minutes before the spacecraft finally crossed that boundary. Just inside the magnetosphere, the proton and electron intensities, and changes in these intensities, resembled those measured by Voyager 1 (*4*); however, starting at 0920 spacecraft event time (SCET)

 0036-8075/82/0129-0577$01.00/0